Cement & Concrete Composites 30 (2008) 535–543

Contents lists available at ScienceDirect

Cement & Concrete Composites

journal homepage: www.elsevier.com/locate/cemconcomp

Corrosion process and abatement in reinforced concrete wrapped by fiber reinforced polymer

Lisa K. Spainhour *, Isaac A. Wootton

Department of Civil and Environmental Engineering, FAMU-FSU College of Engineering, 2525 Pottsdamer Street, Tallahassee, FL 32310-6046, United States

A R T I C L E I N F O

Article history:
Received 24 July 2006
Received in revised form 30 January 2008
Accepted 15 February 2008
Available online 4 March 2008

Keywords:
Carbon fiber reinforced polymer
Corrosion
Steel-reinforced concrete
Epoxy

A B S T R A C T

The corrosion performance of steel reinforcement embedded in concrete samples encased by carbon fiber reinforced polymer (CFRP) wraps was investigated experimentally. Concrete samples were wrapped with 0–3 fabric layers impregnated with one of two different epoxies. To accelerate corrosion, samples were subjected to an impressed current and a high salinity solution. Current flow measurements dynamically monitored corrosion activity during exposure, while reinforcement mass losses were measured following exposure. Theoretical predictions of total mass loss were compared with actual corrosion mass loss values. Test results indicated that CFRP wrapped specimens had prolonged test life, decreased reinforcement mass loss, and lower corrosion rates. The performance of wrapped specimens was superior to that of either control samples or those coated only with epoxy. Results indicated that the level of corrosion abatement provided by the CFRP wraps was influenced both by the type of epoxy used and the number of wrap layers.

1. Introduction

The use of carbon fiber reinforced polymer (CFRP) composite wraps to delay the onset of reinforcement corrosion and reduce the rate of corrosion in concrete samples exposed to an aggressive chloride environment was experimentally investigated. Additionally, the effects of number of wrap layers and the type of impregnating epoxy were considered. According to the American Concrete Institute, composites are particularly suitable for rehabilitating structures because they are lightweight, corrosion-resistant, customizable, and have high tensile strength [1]. The application of CFRP materials specifically to protect reinforced concrete structures from corrosion, specifically bridge foundations (i.e. piers and piles) exposed to harsh chloride environments, has not been widely studied, nor has the effect of different impregnating systems.

2. Background

2.1. Related research

The corrosion of steel in a concrete environment is an electrochemical process requiring an anode, a cathode, an electrolyte, and a contact between the anode and cathode. Ions present in salt water that leach into concrete can provide a means for active reinforcement corrosion. Normally, concrete cover provides both chemical and physical barriers to corrosion of embedded reinforcing steel. Fig. 1 shows a model for the natural corrosion process of steel encased by concrete adapted from Bentur et al. [2]. In this natural corrosion model, the initiation stage describes the time period required for the conditions for steel depassivation to occur; that is, the time where aggressive agents, such as chloride ions, migrate through the concrete to the surface of the steel and buildup sufficient concentration to breakdown the steel passivation layer. The corrosion rates at the propagation stage, or stage where active corrosion has already initiated, are shown to accelerate significantly once the concrete cover has cracked. Depending on their composition and degree of hydration, the products of the corrosion of iron can take up a volume as much as six times that of the original iron [3]. When this expansive process occurs in reinforced concrete, it induces internal stresses in concrete that can eventually lead to spalling or delamination of the concrete around reinforcing steel. The cross sectional area of the steel can be significantly reduced, particularly during the later stage of corrosion propagation.

If the concrete can be kept from deteriorating, the migration of undesirable ions into concrete could be slowed down, and it would follow that the rate of corrosion would decrease. It has been shown that, under short-term exposure conditions, carbon fiber wraps effect the absorption of water into concrete, reducing infiltration at the surface and eliminating the penetration of water into the interior of specimens [4]. A study to evaluate steel reinforcement

* Corresponding author. Tel.: +1 850 410 6123; fax: +1 850 410 6142.
E-mail address: spainhou@eng.fsu.edu (L.K. Spainhour).

0958-9465/$ - see front matter © 2008 Elsevier Ltd. All rights reserved.
doi:10.1016/j.cemconcomp.2008.02.004

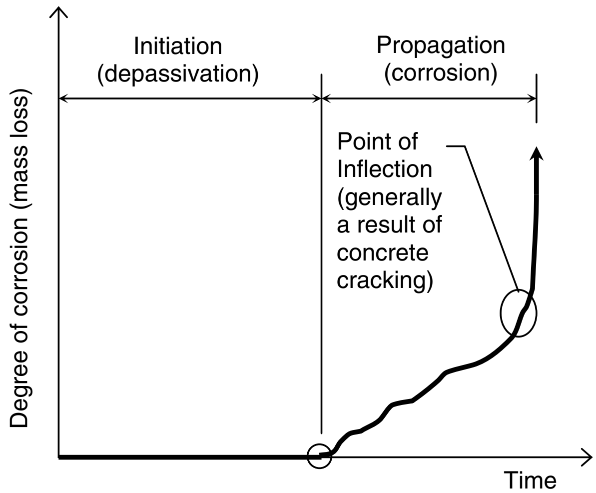

Fig. 1. Corrosion process model for steel in concrete.

corrosion and the properties of concrete specimens coated with waterproofing coatings concluded that the water absorption capacity was a simple physical property that could be considered to predict the protection performance of coating systems against corrosion [5].

Research by Debaiky et al. [6–8] on CFRP wrapped column stubs showed that CFRP wrapping reduced corrosion activity in the reinforcing steel even under harsh conditions, as measured by decreased corrosion current density, decreased mass loss, and reduced chloride diffusion from external sources. It was found that increasing the number of CFRP layers did not significantly enhance the protection. The research concluded that the CFRP wraps applied over corrosion-damaged reinforced concrete columns will decrease the corrosion rate of the reinforcement and restore the structural integrity of the column. A combination of electrochemical chloride extraction and wrapping was found to provide the best protection against future corrosion.

Researchers at the University of Toronto and colleagues conducted several studies into the behavior of reinforced concrete columns wrapped with CFRP and GFRP sheets before and after being subjected accelerated corrosion [9,10]. In one study, large-scale circular concrete columns were subjected to an accelerated corrosion regime then repaired using CFRP sheets [9]. In that study, the repairs were shown to greatly improve the strength and ductility of repaired corroded members and reduced the rate of post-repair corrosion. Moreover, subjecting the repaired column to extensive, post-repair corrosion resulted in no loss of strength or stiffness and only a slight reduction in the ductility of the repaired member. In a second study, GFRP wraps were used in combination with grouting the voids between the jacket and the original surface of the specimen [10]. Different types of diffusion barriers were used to protect the GFRP wraps from exposure to alkali activity of the fresh grout, and to reduce the supply of oxygen and water to the mechanism of corrosion. Increasing the number of GFRP layers and providing sufficient wrap anchorage was found to improve performance, while prestressing with expansive grouts compromised performance.

Suh et al. [11] examined the effect of CFRP and GFRP wraps on scale model prestressed piles exposed to simulated tidal cycles for nearly three years. This study also showed that corrosion rates decreased in wrapped specimens and while increasing in control specimens. Metal losses were also much lower in wrapped specimens compared with controls. The results showed that the FRP-concrete bond was largely unaffected by exposure and both CFRP and GFRP-repaired specimens significantly outperformed the controls.

2.2. Theory

The objective of this research is to investigate the effect of various configurations of CFRP wraps and two-part epoxies on the corrosion-induced mass loss of steel rebar in reinforced concrete. One experimental technique to expedite reinforcing bar corrosion in concrete samples uses exposure to aggressive conditions while forcing corrosion activity through galvanostatic corrosion. In this technique, direct current is impressed into the steel reinforcement so that it becomes the anode while an auxiliary element serves as a cathode. When a constant voltage is maintained between the anode and cathode, the current level is proportional to the speed of the corrosion process. An accurate representation of the corrosion current activity and speed of corrosion acceleration is the corrosion current density i_{corr}, expressed as current divided by the total surface area of the polarized steel ($\mu A/cm^2$). The amount of corrosion is related to the electrical energy consumed, which is a function of voltage, amperage, and time interval. The amount of corrosion can be estimated using Eq. (1) which is based on Faraday's Law.

$$\Delta m_{\text{theoretical}} = \frac{t \cdot i \cdot M}{z \cdot F}, \tag{1}$$

where t is the time (s), i the current (A), M the atomic weight of iron (55.847 g/mol), z the ion charge (assumed 2 for $Fe \rightarrow Fe^{2+} + 2e^-$) and F the Faraday's constant (96,487 A s).

This technique was successfully used by researchers studying the bond behavior of corroded reinforcing bars in concrete samples who found that when current was passed through a bar suspended in salt solution the correlation between actual and predicted mass loss was almost perfect [12]. Furthermore, they found that when a bar was embedded in concrete, mass loss based on Faraday's law overestimated the actual mass loss, but that, by passing external current, it is still possible to induce predetermined accelerated corrosion. In a similar manner, Debaiky et al. [7] used Faraday's equation to accurately estimate mass loss in CFRP wrapped reinforced concrete samples subject to an impressed current.

3. Experimental program

3.1. Materials

Portland Cement Association guidelines for the proportioning of normal concrete mixtures for small jobs were followed to establish the concrete mix design for this study [13]. Concrete mix proportions were 1:2.5:1.5:0.5 by volume of cement, wet fine aggregate, wet coarse aggregate, and water, respectively. The 28 day compressive strength was 24.5 MPa (3560 psi), which is within the anticipated range of 20.7–34.4 MPa (3000–5000 psi) for the mix design. The CFRP wraps consisted of a unidirectional carbon fabric (12,000 filaments/yarn, 4 yarns/cm width, ply thickness of 0.55 mm (0.022 in.)) embedded in a thermoset epoxy. The fabric has a tensile strength of 3.1 GPa (450 ksi), modulus within 221–241 GPa (32–35 Msi), and an areal weight of approximately 340 g/m^2 (0.07 psf) according to manufacturer's literature [14]. Two different brands or types of epoxy were tested. Each of the two-part systems incorporated a clear, pale amber, low-viscosity (approximately 1 $N s/m^2$ at 22 °C, according to manufacturer's data) liquid epoxy resin combined with an aromatic hydrocarbon-blend curing agent. The two epoxies were selected because of their adherence to concrete and carbon fibers and because of their resistance to moisture.

The first epoxy, West System 105 (referred to henceforth as WS), is a marine grade epoxy designed specifically for reinforcing fabrics [15]. Product literature states that this epoxy offers excellent wet out and adhesion to fiberglass, carbon, and aramid fabrics. The resin is described as a Bisphenol A based epoxy resin, and the hardener is described as a modified aliphatic polyamine. This epoxy dries to a hard, clear finish and does not require a polyester gelcoat; however, a clear coat of epoxy on the exterior surface is recommended.

The second epoxy, Sikagard 62 (referred to henceforth as SG), is a thick, gray epoxy designed for use as a thick, corrosion-resistant, moisture-insensitive protective coating [16]. Product literature states that this epoxy may be applied to concrete or carbon laminates, and offers long-term protection from chlorides and water ingress. The resin is described as a modified epoxy resin of the epichlorohydrin Bisphenol A type containing suitable viscosity control agents. The hardener is described as a proprietary blend of aliphatic and cyclic amines, containing suitable viscosity control agents, pigments, and accelerators.

3.2. Specimen preparation

Scale-model concrete test specimens were cast in the form of cylindrical "lollipop" samples. Each sample was 51 mm (2 in.) in diameter, 102 mm (4 in.) in height, and contained a single 12.7 mm (1/2 in.) diameter steel reinforcing bar. The reinforcement was cleaned of surface rust prior to casting, and secured such that it protruded from the top of the mold by 19 mm (3/4 in.) thus providing a uniform concrete cover of 19 mm (3/4 in.) at the sides and bottom. The CFRP wraps were applied to samples in a hand lay-up procedure. An initial coat of epoxy was applied to the bottom and sides of the samples, followed by the application of successive wetted fabric layers then followed by a final clear coat of epoxy. The CFRP wraps were applied with the fiber strong axis aligned in the hoop (circumference) direction. Samples were cured at room temperature for 24 h between layer applications, and for 28 days before testing. The careful sample preparation was intended to ensure optimum sample response, rather than mimic field practice. Each category shown in Table 1 consisted of three samples and represents a treatment variation. Surface coating options fell into three main groups: control samples that were untreated, those that were only coated with epoxy, and finally those that were wrapped with one to three CFRP composite wrap layers.

3.3. Exposure conditions

Specimens, initially dry, were placed in a tank and immersed, to a depth of approximately 95 mm (3–3/4 in.), in a 5% NaCl solution at a room temperature of approximately 24 °C (75 F). Fig. 2a shows a schematic of the test configuration, with samples connected to a 12-volt DC power supply, thus impressing a current such that the reinforcing bars are anodic; Fig. 2b shows a photograph of the actual test setup.

The high salinity and the impressed current were both used to create an especially aggressive environment by providing an abundance of chloride ions and by stimulating an increased flow of electrons, respectively. The initial electrical resistivity of the CFRP wraps was not found to differ significantly between sample categories nor did the initial electrical resistance in each of the parallel circuits. Current passing through the CFRP wraps was not expected to greatly affect the wrap properties. To maintain a consistent testing environment over the 50-day experimental test period, the salt water in the tank was replaced weekly, electrodes were cleaned daily and the wiring and electrical connections checked twice a day.

Table 1
Sample surface treatments

Category name	Epoxy type	CFRP layers	Average CFRP thickness (mm)
CTRL	None	0	N/A
WS0	West System	0	N/A
WS1	West System	1	1.1
WS2	West System	2	2.3
WS3	West System	3	3.4
SG0	Sikagard	0	N/A
SG1	Sikagard	1	1.8
SG2	Sikagard	2	2.6
SG3	Sikagard	3	4.1

3.4. Corrosion monitoring and testing

3.4.1. Current measurements

The electrical energy consumption of each sample was monitored regularly by measuring current flow. Approximately every 12 h, corrosion current measurements were recorded in each sample using a voltmeter just after turning off the power supply. Switches, as shown in Fig. 2, allowed each circuit to be isolated during data collection. Current readings, expressed in terms of the corrosion current density i_{corr}, are shown in Figs. 3 and 4 for the 50-day test period.

A current reading in excess of 320 mA (corrosion current density > 8000 $\mu A/cm^2$) was designated as a condition of sample failure, and subsequently the sample was disconnected and examined. This failure criterion was selected due to the potential hazard posed to electrical circuitry from excessive current flow. Typically, a current spike or rapid increase in the corrosion current density was observed preceding sample failure and indicated that a sharp reduction in resistance between the sample reinforcement and the electrodes in the tank had occurred. This circuit shorting, caused by concrete cracking, suggested that enough cracks had formed in a sample that failure was imminent. These current spikes, clearly discernible in Figs. 3 and 4, revealed the rapid acceleration in corrosion rate that occurred once the reinforcement protection had been compromised. Current flow values and the known time intervals between data collection were input into the equation given in the background section. In this way, Faraday's law was used to approximate theoretical mass loss or amount of steel consumed over time. Note that, for most samples, corrosion current density was in the range of 1000–2000 $\mu A/cm^2$ prior to current spike and sample failure, which is approximately 10–20 times the maximum natural current density of around 100 $\mu A/cm^2$.

3.4.2. Sample examinations

Samples were visually inspected for cracks daily and, if being removed from the tank due to a spike in current flow, were examined to see if the concrete exhibited significant cracking (concrete failure), and/or the wrap tore or otherwise failed (wrap failure). Samples were also removed from testing if the steel began to experience excessive corrosion and cross sectional loss in the exposed portion of the reinforcement (rebar failure). At the end of the accelerated corrosion test period, samples which had not yet failed were disconnected (end of test). Fig. 5 shows various sample failures, including (a) untreated control sample showing concrete failure; (b) concrete failure accompanied by ripping of the wrap; and (c) wrap failure with intact concrete accompanied by delamination of outer wrap layer. Fig. 6 gives, for each of the samples tested, the reason for sample removal and the total length of accelerated corrosion exposure.

Following exposure, reinforcing bars were extracted from each of the concrete samples for chemical cleaning. The reinforcing bar was placed in a 10% solution of muriatic acid for a week to remove all corrosion products and remaining concrete. The bars were then weighed to the nearest 0.01 g. Once clean, the reinforcing bars were weighed and the final values compared with initial bar weights to determine experimental or actual mass loss. Fig. 7 shows several samples of the corroded bars after cleaning. Note

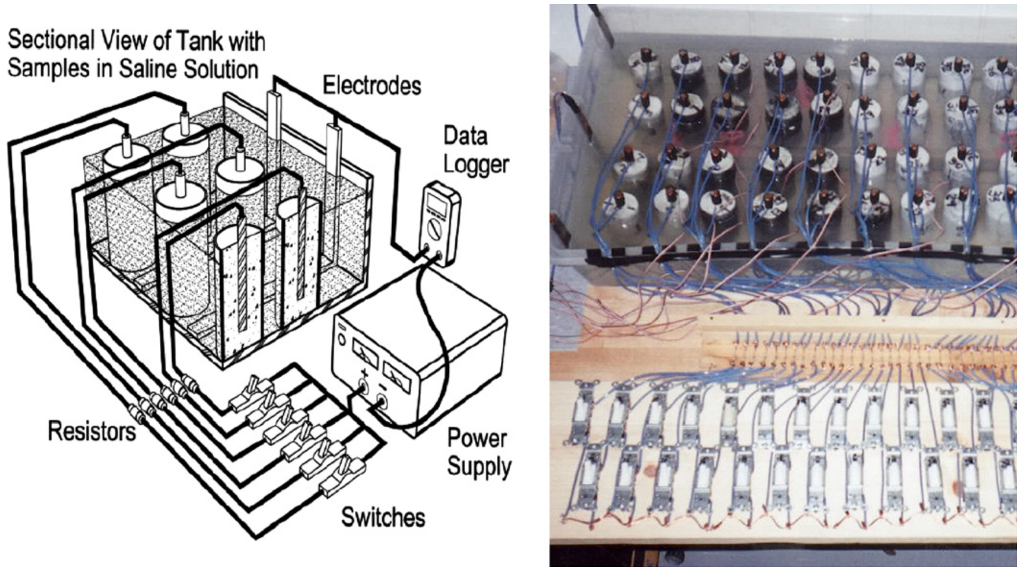

Fig. 2. Accelerated corrosion test configuration.

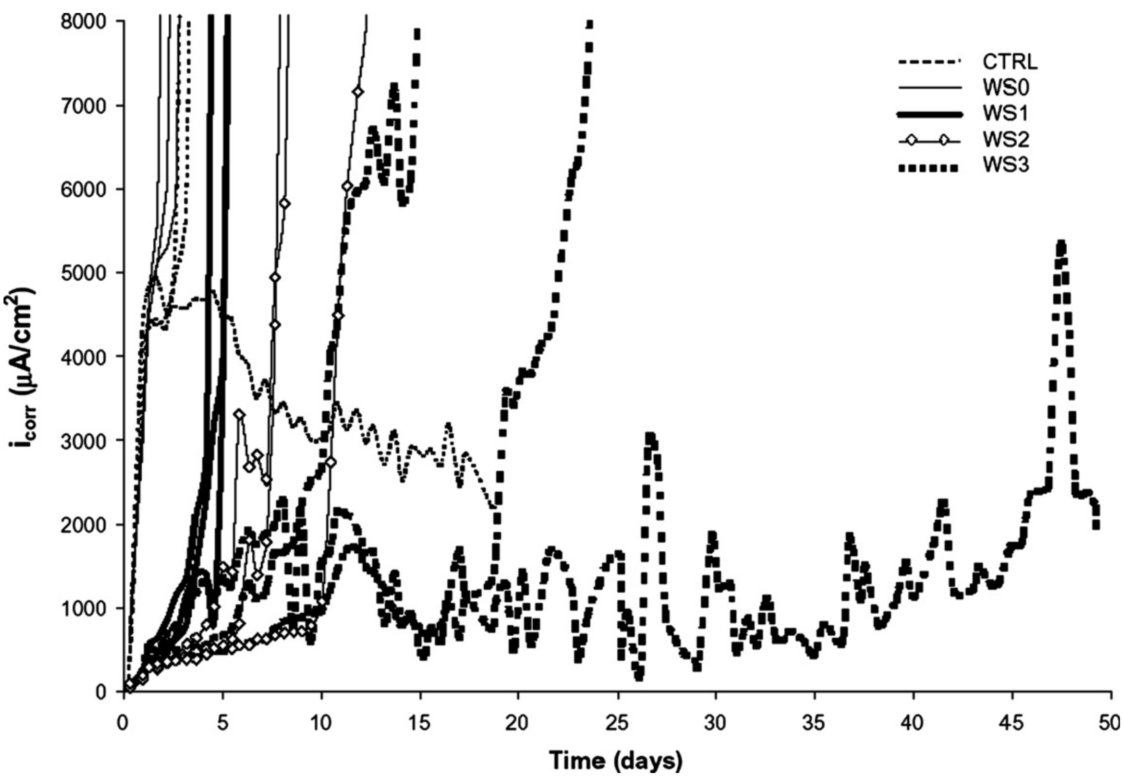

Fig. 3. Corrosion current density versus time for WS samples.

that most show uniform or increasing corrosion toward the bottom with some evidence of section loss in the exposed portion of the rebar above the concrete surface.

4. Results and discussion

4.1. Comparison of final theoretical and actual corrosion mass loss

The cumulative theoretical mass loss was compared to the actual mass loss for each sample. Fig. 8 plots the actual versus predicted total mass loss, grouped by treatment category, for all the samples. The trend lines shown were calculated using linear regression analysis. When current is passed through a bare steel bar exposed to water, chlorides, and oxygen, the correlation between actual and predicted mass loss should theoretically be equal to 1. This condition is found when a steel bar is suspended in a saline solution. However, once the steel bars are embedded in concrete this correlation is expected to change somewhat because of the effect of the concrete on current flow [12]. As shown in Fig. 8, it was found that in general the calculated mass loss

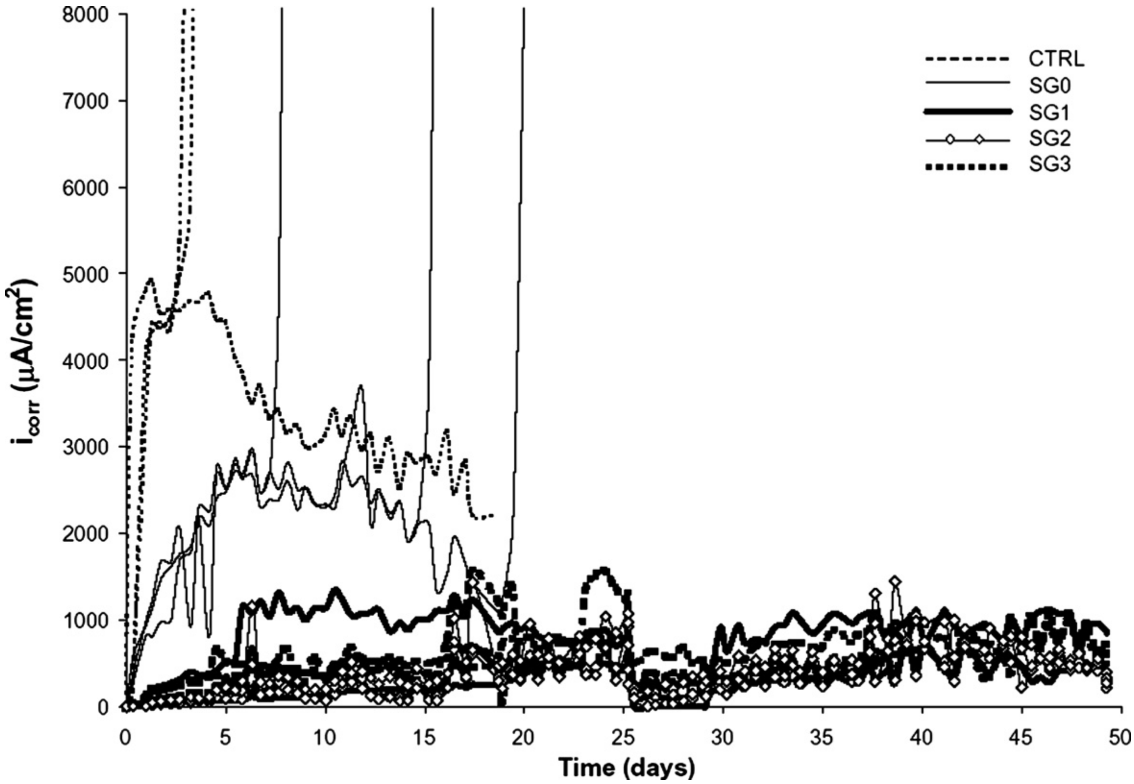

Fig. 4. Corrosion current density versus time for SG samples.

Fig. 5. Example specimen failures.

under predicts the actual amount of corrosion mass loss; however, the results are actually well correlated. Trendlines, given in Fig. 8, include all of the samples of a particular treatment group, except in the case of WS samples, where an adjusted trendline (outliner samples removed) is also given. A more detailed explanation of the adjusted trendline is given in the latter portion of this section. As given in the figure, data points fit the trend lines quite well with high R^2 values. Possible factors that may have lead to differences between actual and theoretical mass loss values are:

- Natural corrosion, that would not have been accounted for in the theoretical mass loss predictions, would have occurred while samples were disconnected from the impressed current circuitry (samples were disconnected from the circuit for approximately 2–2.5 h a day for maintenance and testing, and samples that failed early were removed from the tank but were not cleaned and weighed until the end of the test).
- The electrical properties of the minerals in the concrete, the CFRP wraps, and deposits in the salt solution.
- A certain amount of energy is needed to initiate corrosion in steel bars embedded in concrete, as reasoned by Auyeung et al. [12]. Theoretical predictions of mass loss assume that the corrosion begins as soon as the electrical energy is applied; however, when encased by concrete the initial availability of chlorides and oxygen is limited. Assuming corrosion begins as soon as energy is applied would lead to higher predicted corrosion mass loss.
- Assumed composition of the reinforcing steel. Theoretical mass loss calculations, based on Faraday's law, assume that the bar is made of pure iron when the chemical composition of reinforcing steel commonly includes around 0.50% carbon. Assuming an iron composition would lead to higher predicted corrosion mass loss.

The integrity of the concrete in the sample also appears to play a role in the magnitude of the actual corrosion, and thus in the percent error between actual and theoretical values. This can be seen in Fig. 9, which shows the percent error between the predicted and actual total corrosion mass loss, grouped by treatment style for each of the samples. It is expected that concrete that is sound and not deteriorated will contain reinforcement that has undergone less corrosion than predicted. In Fig. 9 it can be seen that, on average, samples with 2 or more CFRP wraps generally have negative percent errors. A negative value means that theoretical mass loss is greater than the actual mass loss (less corrosion than predicted). This implies that some of the current did not contribute to corrosion and may have been consumed while passing through the concrete and wrap. Conversely, it is reasoned that concrete that is deteriorated from corrosion damage will have cracks and decreased resistance, resulting in corrosion that is closer to predicted levels. Samples with short test lives experienced corrosion

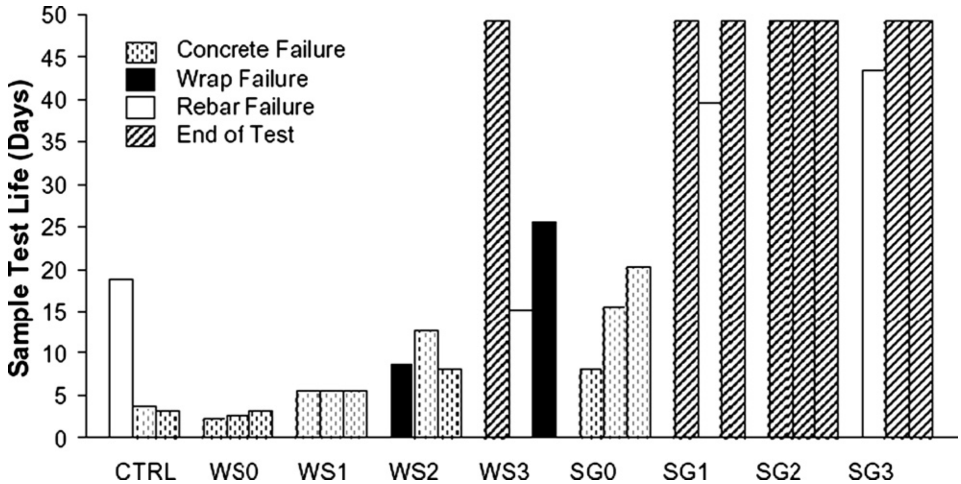

Fig. 6. Length of sample exposure and cause for ending exposure.

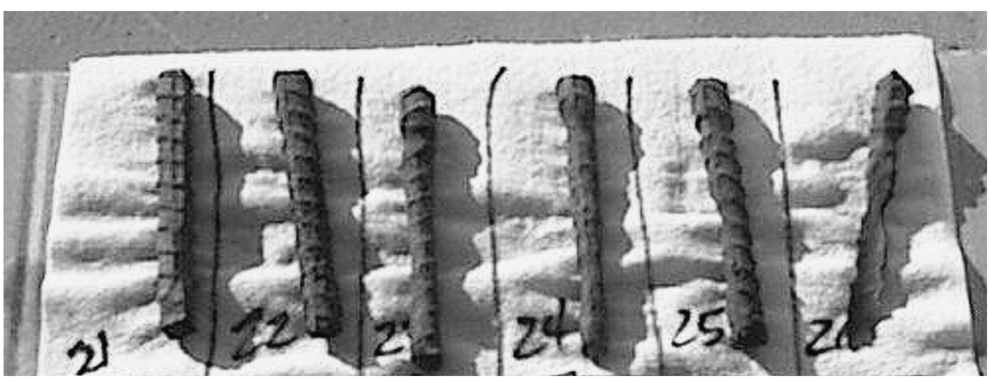

Fig. 7. Sample rebars following exposure and cleaning.

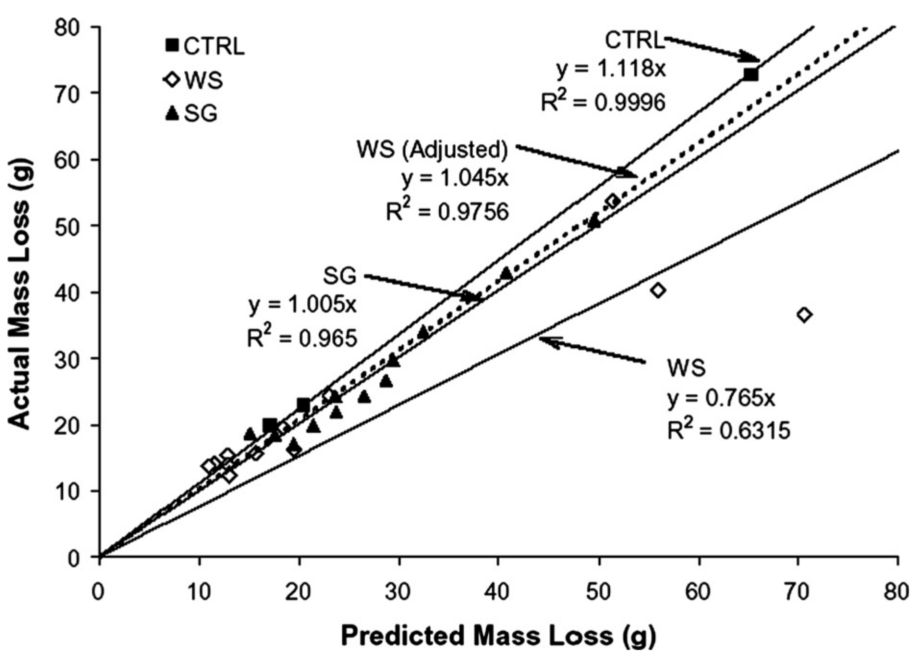

Fig. 8. Actual versus predicted total mass loss.

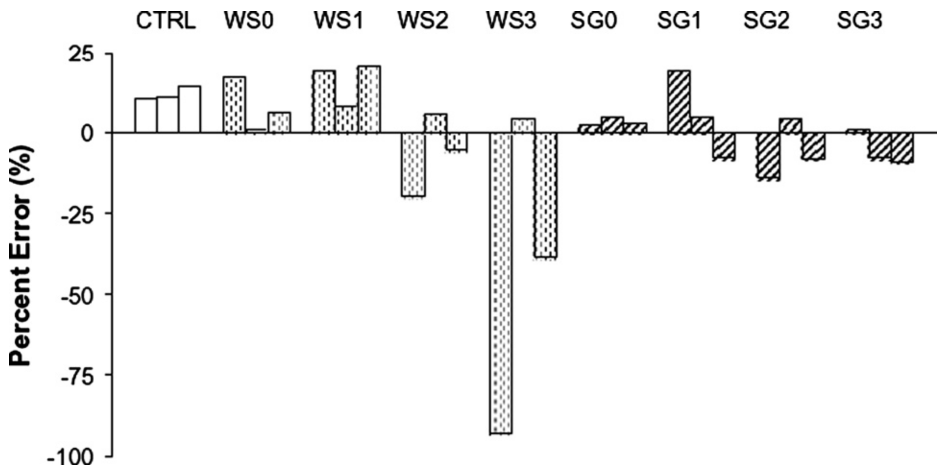

Fig. 9. Percent error between actual and predicted total mass loss.

damage at a relatively early stage and generally show positive percent errors (more corrosion than predicted). Natural corrosion that was unaccounted for while these samples awaited destructive testing also likely contributed to the positive errors and underprediction of corrosion.

In Figs. 8 and 9, it is apparent that, while most samples have relatively good correlation between actual and theoretical mass loss, with less than twelve percent error in the slope of the trendlines, two samples have a much higher percent error. Although no specific experimental cause could be identified for the high rate of error in these aberrant samples, it is worth noting that both are WS3 wrapped samples that exhibited less corrosion than predicted by the current flow measurements. However, because the error in these samples was so extreme, they were examined specifically for fit. Using a technique identified by Vining, these two values were identified as outliers [17]. The relationship for the remaining WS data, with the two outlier samples removed from the data set, is shown in Fig. 8 as "WM (Adjusted)." The adjusted trendline resembles the other cases more closely follows the expected behavior, and has a much higher R^2 value than the original trendline.

In this study, the cumulative theoretical mass loss values based on Faraday's law correlate well to actual recorded mass loss values, regardless of sample style. This indicates that neither the wraps (number of layers and layer orientation) nor the epoxy (type and thickness) has a significant effect on the validity of the theoretical predictions. In addition, because of the strong correlation, the theoretical mass loss values can be used to examine the corrosion behavior of the samples over time.

4.2. Accumulative theoretical corrosion mass loss over time

Theoretical mass loss predictions, computed using Faraday's law and corrosion current measurements, were used to examine accumulative mass loss over time, as shown in Figs. 10 and 11. The natural corrosion process model for steel in concrete, exposed to an aggressive environment, has an exponential tendency after active corrosion has been initiated (see Fig. 1). In this experiment, where an impressed current was used to accelerate the corrosion process, the exponential nature is still discernible. Slopes of the curves in Figs. 10 and 11 indicate the rates of corrosion, or predicted corrosion mass loss over time. The initiation stage, which is the time to onset of corrosion mass loss, is much shorter than what would be expected under natural corrosion conditions. For the conditions of this experiment, the initiation stage ranges from less than a half a day up to four days. In numerous cases an inflection point is distinguishable during the propagation stage, or active corrosion stage, where the corrosion mass loss rate rapidly accelerated.

A comparison of the predicted mass loss versus time graphs clearly reveals that the CFRP wraps are able to delay to onset of corrosion, lengthen sample test lives, and lower overall rates of corrosion mass loss. It is also clear that samples treated using the WS epoxy do not perform as well as samples treated using SG epoxy. Fig. 10 illustrates the benefits, regarding corrosion abatement, of the WS wraps while Fig. 11 reveals the benefits, again in regard to abating corrosion, of both the SG epoxy coating and the SG wraps individually, with the SG epoxy itself appearing to have a notable role in lowering the rates of corrosion.

In Fig. 10 it can be seen that the WS epoxy coating has no effect on the onset or rate of corrosion. The CFRP wraps with the WS epoxy delay the onset of corrosion, albeit minimally, from less than half a day in control and epoxy coated samples to around a day for the rest of the WS wrapped samples. Thus, the onset of corrosion for WS samples takes over twice as long when samples are wrapped. For WS samples, a correlation seems apparent between the number of wrap layers and sample performance. In general, with the introduction of each additional wrap layer, the average length of time to the point of inflection doubles. As shown in Fig. 10, the point of inflection occurs within a day for control and epoxy coated samples, between 4 and 5 days for samples with 1 wrap layer, between 6 and 10 days for samples with two wrap layers, and between 10 and 45 days for samples with three wrap layers. The improved performance of samples with more wraps is thought to be attributed to both the amplified circumferential confinement provided by the greater number of CFRP layers, and the increased ability to inhibit the passage of chlorides. Confinement of the concrete is the result of a CFRP wrap opposing volume increases, or hoop dilatation, which is caused by the building up of expansive corrosion products in a sample. Circumferential confinement of the concrete by the wraps would slow deterioration from cracking and spalling, thereby explaining the lower corrosion rates.

In the case of SG samples, an epoxy coating was able to delay the onset of corrosion by a factor of 2, as seen in Fig. 11. The effect of the CFRP wraps at delaying the onset of corrosion is even more significant for SG samples with the onset of corrosion taking 4–8 times longer when samples are wrapped. However, for SG samples, there is not a clear distinction between the performances of more than one wrap layer, nor did any samples experience a point of inflection within the duration of the test. It is probable that, in conjunction with the SG epoxy, even a single CFRP layer is enough to inhibit the passage of salt water, protect the concrete from deterioration and considerably slow the overall corrosion rate.

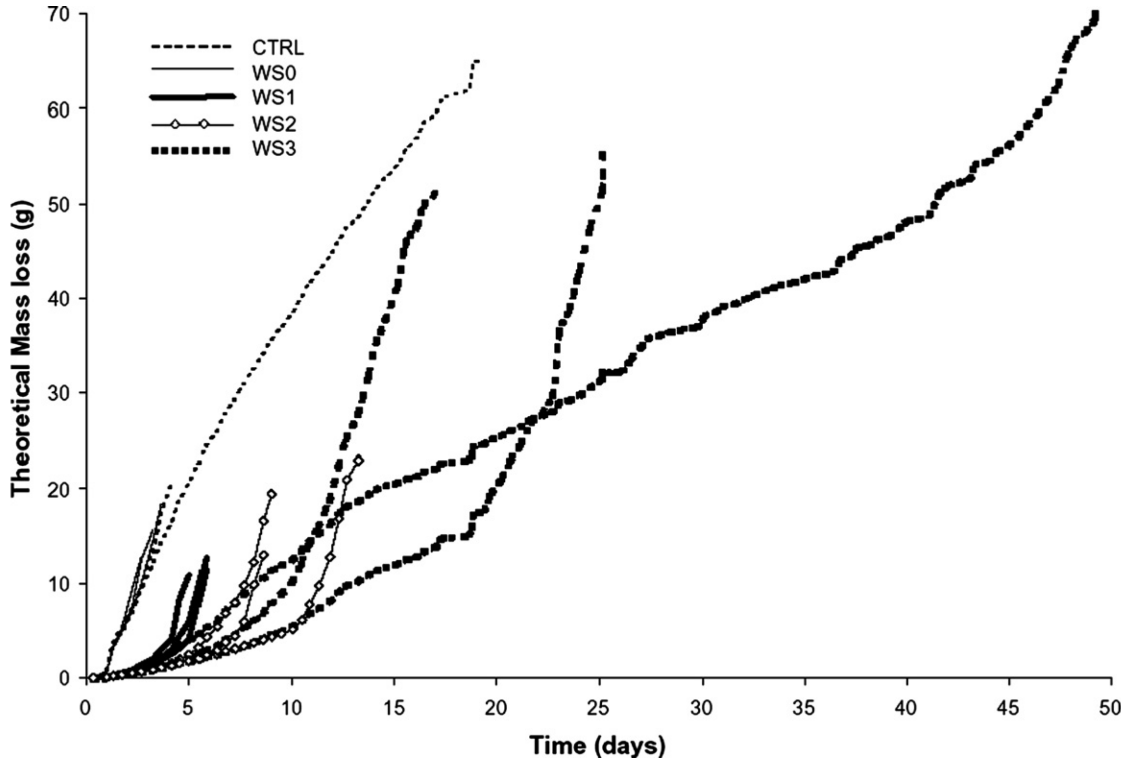

Fig. 10. Predicted mass loss versus time for WS samples.

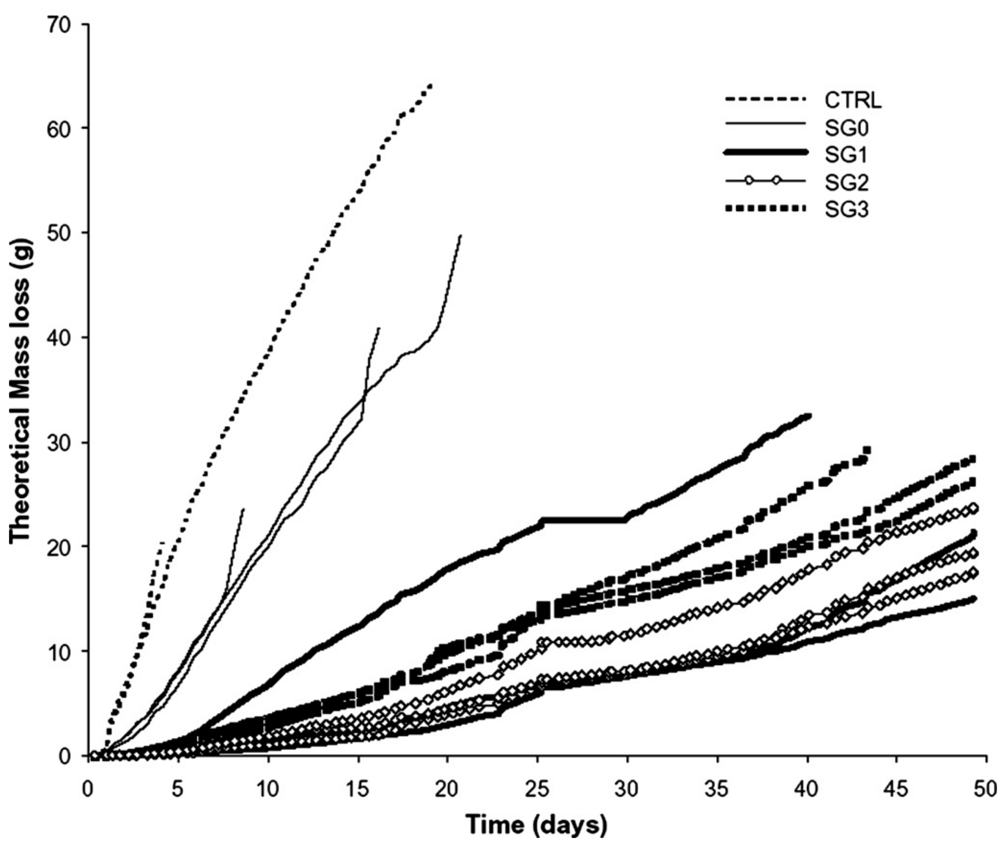

Fig. 11. Predicted mass loss versus time for SG samples.

The superior performance of the SG samples becomes evident with a simple comparison of the data in Figs. 10 and 11. To sustain 10 g of corrosion mass loss takes WS samples only from 5 to 13 days while SG wrapped samples takes from 13 to 38 days, or up to eight times longer to reach the same level of corrosion mass loss. Test results suggest that the SG epoxy maintains the integrity of the composite wrap under the test conditions longer than the WS epoxy does, thereby providing a longer period of protection to the underlying concrete and embedded steel bars. Preserving the integrity of the wraps is attributed to the suitability of the epoxy to aggressive corrosive conditions, as found in this test. Although the average thickness of the WS samples with three wraps is greater than the average thickness of the SG samples with either 1 or 2 wraps, the SG samples with even a single wrap layer lasts longer and has lower amounts of corrosion mass loss when examined within the same period of exposure.

5. Conclusions

A comparison of the accumulative predicted corrosion mass loss over time to actual mass loss was performed for control samples and samples treated with one of two different types of epoxies. Within groups, samples were treated with an epoxy coating or with a CFRP wrap having from one to three layers. The research described herein is intended to be an accelerated study and not to replicate natural field conditions or treatments; the results and conclusions are limited to the information obtained from the experimental studies. Based on the observations made during the experimental investigation as reported in this paper the following conclusions can be drawn:

- For samples with or without CFRP wraps, the predicted mass loss based on Faraday's law correlates reasonably well with actual mass loss measured. Although the concrete and other factors may slightly affect the theoretical predictions, the calculated mass loss can be used to examine mass loss over time.
- CFRP wrapping is effective at abating reinforcement corrosion by delaying the onset of corrosion, lengthening sample test lives and reducing the rate of corrosion mass loss.
- Epoxy type is a significant factor affecting the performance and corrosion resistance of a CFRP wrap. One type of epoxy used for the CFRP wraps in this experiment (SG) is considerably more effective at delaying the onset and reducing the rate of corrosion in samples than another (WS). However, epoxy alone is not effective at abating reinforcement corrosion.
- In samples with the WS epoxy, it was found that increasing the number of wrap layers, and thus the ability to develop circumferential confinement, improved a sample's performance.

Results indicate that the level of corrosion abatement provided by the CFRP wraps was influenced both by the type of epoxy used and the number of wrap layers. This finding supports a claim that, to a certain extent, the suitability of the epoxy and not the thickness of the wrap is the primary performance factor in regards to the corrosion protection provided by a CFRP composite wrap. However, even the better performing epoxy alone is not sufficient to significantly improve performance, without at least one carbon fabric layer, while additional CFRP layers improved sample performance with the poorer performing epoxy.

References

[1] Guide for the design and construction of externally bonded FRP systems for strengthening concrete structures. ACI 440.2R-02. Committee 440. Farmington Hills, MI: American Concrete Institute; 2002.
[2] Bentur A, Diamond S, Berke NS. Steel corrosion in concrete. London: E&FN Spon; 1997.
[3] Bertolini L, Elsener B, Pedeferri P, Polder R. Corrosion of steel in concrete: prevention, diagnosis, repair. Weinheim, Germany: Wiley-VCH; 2004.
[4] Spainhour LK, Thompson IM. Effect of carbon fiber jackets on reinforced concrete columns exposed to a simulated tidal zone. Fiber composites in infrastructure. In: Proceedings of the 2nd international conference on composites in infrastructure, ICCI '98, vol. 1; 1998. p. 426–39.
[5] Al-Zahrani MM, Al-Dulaijan SU, Ibrahim M, Saricimen H, Sharif FM. Effect of waterproofing coatings on steel reinforcement corrosion and physical properties of concrete. Cement Concrete Compos 2002;24(1): 127–37.
[6] Debaiky AS, Green MF, Hope BB. Corrosion of FRP-wrapped RC cylinders: long term study under sever environmental exposure. In: Presented at 5th international conference on fibre reinforced polymers for reinforced concrete structures. Cambridge; 2001.
[7] Debaiky AS, Green MF, Hope BB. CFRP wraps for corrosion control and rehabilitation of reinforced concrete columns. ACI Mater J 2002;99(2): 129–37.
[8] Debaiky AS, Green MF, Hope BB. Long-term monitoring of carbon fiber-reinforced polymer-wrapped reinforced concrete columns under sever environment. ACI Struct J 2006;103(6):865–73.
[9] Lee C, Bonacci JF, Thomas MDA, Maalej M, Khajehpour S, Hearn N. Accelerated corrosion and repair of reinforced concrete columns using carbon fibre reinforced polymer sheets. Canadian J Civil Eng 2000;27:941–8.
[10] Pantazopoulou SJ, Bonacci JF, Sheikh S, Thomas MDA, Hearn N. Repair of corrosion-damaged columns with FRP wraps. J Compos Construct 2001;5(1):3–11.
[11] Suh K, Mullins G, Sen R. Effectiveness of fiber-reinforced polymer in reducing corrosion in marine environment. ACI Struct J 2007;104(1):76–83.
[12] Auyeung Y, Balaguru P, Chung L. Bond behavior of corroded reinforcement bars. ACI Mater J 2000;97(2):214–20.
[13] Portland Cement Association. Design and control of concrete mixtures. 13th ed. Skokie, Illinois; 1998.
[14] Product Data Sheet. Fabric 12K T250, Amoco polymers. Alpharetta, GA; 1996.
[15] West System Technical Manual and Product Guide. Bay City, MI: Gougeon Brothers Inc.; 1994.
[16] Sikagard 62 Material Safety Data Sheet. Marion, OH: Sika Corporation; 1996.
[17] Vining GG. Statistical methods for engineers. Duxbury Press; 1998.